Therapeutics, Targets, and Chemical Biology

Cancer Research

Feed-Forward Reciprocal Activation of PAFR and STAT3 Regulates Epithelial–Mesenchymal Transition in Non–Small Cell Lung Cancer

Jie Chen[1], Tian Lan[1,2], Weimin Zhang[1], Lijia Dong[1], Nan Kang[1], Shumin Zhang[1], Ming Fu[1], Bing Liu[3], Kangtai Liu[4], and Qimin Zhan[1]

Abstract

Platelet-activating factor receptor (PAFR), a G-protein–coupled receptor, has been implicated in tumorigenesis, but its contributions to metastatic progression have not been investigated. Here, we show that PAFR is overexpressed in non–small cell lung cancer (NSCLC) as well as in breast, colorectal, and gastric carcinomas. Expression of PAFR correlates closely with clinical stages, survival time, and distant metastasis. In human NSCLC cells, activation of the PAF/PAFR signaling axis accentuated malignant character, including by stimulating epithelial–mesenchymal transition (EMT). In contrast, silencing PAFR in aggressive NSCLC cells inhibited these effects. Mechanistic investigations showed that PAFR stimulated EMT by activating STAT3 via upregulation of G-protein–dependent SRC or JAK2 kinase activity. Notably, STAT3 transcriptionally elevated PAFR expression. Thus, activation of PAFR in NSCLC cells initiated a forward feedback loop responsible for mediating the aggressive malignant character of NSCLC cells *in vitro* and *in vivo*. Reinforcing this reciprocal activation loop, PAF/PAFR signaling also upregulated IL6 expression and thereby STAT3 activation. Overall, our results elucidated an important role for PAFR dysregulation in the pathogenicity of NSCLC and unraveled a forward feedback loop between PAFR and STAT3 that acts to drive the malignant progression of NSCLC. *Cancer Res; 75(19); 4198–210. ©2015 AACR.*

Introduction

Non–small cell lung cancer (NSCLC) ranks among the most frequent cancers in the world. Most patients with very small tumors may already develop distant metastasis, constituting the major cause for death of patients with NSCLC and leading to the failure of targeted chemotherapy (1). NSCLC risk and metastasis are caused by a variety of aberrant molecular change, including the mutational activation of KRAS, PI3K, Akt, or Raf oncoprotein and inactivation of the *PTEN* and *TP53* tumor suppressor genes (2). Nevertheless, the comprehensive mechanisms for NSCLC metastasis remain to be further defined.

G-protein–coupled receptors (GPCR), the largest family of cell-surface molecules, all share a characteristic core composed of seven-transmembrane α-helices, and have a crucial but often not fully appreciated role in cancer progression and metastasis (3). The aberrant overexpression of GPCRs and their autocrine and paracrine activation by agonists released by tumor or microenvironment cells stimulates GPCRs and their signaling networks and subsequently induce tumor metastasis. For example, Nikitenko and colleagues reported that calcitonin receptor–like receptor (CLR), a type of GPCRs, is upregulated in an autocrine loop with its ligand adrenomedullin to promote the progression of clear cell renal cell carcinoma (ccRCC; ref. 4). Lysophosphatidic acid (LPA) has been found to interact with its receptor to drive the uncontrolled growth of ovarian cancer cells in an autocrine fashion (5). Furthermore, the autocrine secretion of neuropeptides such as gastrin-releasing peptide (GRP), endothelin and bradykinin activate their GPCRs to stimulate the progression of various tumors (3).

Platelet-activating factor receptor (PAFR), a type of G protein–coupled receptor and its ligand PAF (6), can regulate diverse cellular functions in various tumors. For example, the activation of PAFR can stimulate various kinases and the downstream signaling pathway to promote melanoma metastasis (7). Inhibition of PAFR activity by its specific inhibitor can effectively block the breast cancer cell growth and invasion *in vitro* (8). Disruption of the PAF/PAFR interaction or knockdown of the expression of PAFR can effectively block the invasion of ovarian tumor cells (9). However, the biologic roles of PAFR in NSCLC metastasis have not been investigated.

Epithelial-to-mesenchymal transition (EMT) is a coordinated molecular and cellular change characterized by a reduction in cell–cell adhesion, apical–basolateral polarity, and epithelial markers such as E-cadherin, as well as an acquisition of motility, spindle-cell shape, and mesenchymal markers such as N-cadherin

[1]State Key Laboratory of Molecular Oncology, Cancer Institute and Hospital, Chinese Academy of Medical Sciences and Peking Union Medical College, Beijing, China. [2]Department of Neurosurgery, Beijing Sanbo Brain Hospital; Capital Medical University, Beijing, China. [3]Department of Pharmacology, School of Pharmacy, Guangdong Pharmaceutical University, Guangzhou, China. [4]National Key Laboratory of Medical Molecular Biology, Institute of Basic Medical Sciences, Peking Union Medical College, Tsinghua University and Chinese Academy of Medical Sciences, Beijing, China.

Note: Supplementary data for this article are available at Cancer Research Online (http://cancerres.aacrjournals.org/).

J. Chen and T. Lan contributed equally to this article.

Corresponding Author: Qimin Zhan, State Key Laboratory of Molecular Oncology, Cancer Institute and Hospital, Chinese Academy of Medical Sciences and Peking Union Medical College, Panjia Yuan Nanli 17, Beijing 100021, China. Phone: 86-10-6776-2694; Fax: 86-10-6771-5058; E-mail: zhanqimin@pumc.edu.cn

doi: 10.1158/0008-5472.CAN-15-1062

and vimentin (10). The EMT process has been well accepted to give rise to the dissemination of single carcinoma cells from primary epithelial tumors (11). It is critically required for cancer progression and metastasis of solid tumors, including NSCLC (12).

In this study, we find that promotion of PAF/PAFR contributes to EMT-induced invasion and metastasis of NSCLC cells. We demonstrate that PAFR induces EMT by activation of the Stat3 pathway, and there exists a feed-forward reciprocal activation between PAFR and Stat3. Especially, the PAF/PAFR axis positively regulates IL6 expression, contributing to persistent Stat3 activation. Taken together, we have made the first demonstration that dysregulation of PAFR and the forward feedback loop between PAFR and Stat3 contributes to malignant progression of NSCLCs.

Materials and Methods

Cell lines and transfection

The normal lung cell lines BEAS-2B (originally purchased from the ATCC) and normal human bronchial/tracheal epithelial cells (NHBE; originally purchased from Lonza) or human NSCLC cell lines H441, H292, H226, Calu-3, A549, H1299, H460, H157, Calu-1, and H23 (originally purchased from the ATCC) were originally maintained in RPMI1640 medium supplemented with 10% FBS, penicillin (100 U/mL), and streptomycin (100 μg/mL). Cells were maintained at 37°C in a humidified 5% CO_2 incubator. All the cell lines were recently authenticated by cellular morphology and the short tandem repeat analysis using the AmpF/STR Identifier Kit (Applied Biosystems). For shRNA experiments, A549 and H460 cells were transfected with the pRetroSuper (pRS; Origene) and pRS vector expressing shRNA for PAFR knockdown (pRS-shPAFR) or pRS vector expressing shRNA for Stat3 knockdown (pRS-shStat3). Transfected cells were selected by 0.5 μg/mL puromycin. Stable cell lines expressing PAFR was generated by transfection of pCMV-PAFR into Calu-3 and H226 cells and cultured for 10 days with 400 μg/mL G418 after infection. Positive clones were then selected and amplified for further analyses. For Stat3 plasmid transfection, A549 and H460 cells (60% confluence, approximately 5×10^6 cells) were transfected with 2 μg of pcDNA3.1-Stat3 (Guangzhou Ribobio Co.) or pcDNA3.1 using Lipofectamine 2000 (Invitrogen) according to the manufacturer's instructions.

Cell proliferation/viability assay

The protocols and reagents used for the MTS assay (detection of cell proliferation/viability) were all strictly according to previous work (13).

Transwell invasion assay

The Transwell invasion assay was performed using the Transwell chamber with a Matrigel-coated filter. A total of 3×10^4 cells to be tested were starved in serum-free and growth factor–free medium for 12 hours and then plated on the top chamber with or without agents as indicated for 24 hours, followed by the removal of cells inside the top chamber with cotton swabs, and the invasive cells on the lower side were fixed, stained with 0.1% crystal violet solution, and counted using a light microscope. The experiment was repeated three times.

Immunoblotting

Total 50 μg of protein extracts were loaded and electrophoresed on 8% to 12% SDS gel and transferred to nitrocellulose membranes. The membranes were subsequently probed with primary antibodies, respectively. All of the first antibodies were diluted at 1:1,000 except for GAPDH at 1:5,000. Antibody binding was detected by enhanced chemiluminescence detection kit (ECL; UK Amersham International plc). Blotting membranes were stripped and reprobed with anti-GAPDH as a loading control.

ELISA

ELISA was done using a human IL6 ELISA kit according to the manufacturer's instruction (R&D Systems). Briefly, the cells were seeded in 12-well plates and cultured to 90% to 100% confluence. Cells were cultured in fresh culture medium in the presence of control solvent or 100 nM PAF. After 24-hour incubation, the supernatants were collected and cell numbers of each well were counted. IL6 in the supernatant (100 μL) was determined and normalized to the remaining cell numbers. The optical densities were read at 490 nm, and the level of IL6 concentration was calculated as pg/mL.

Chromatin immunoprecipitation

Chromatin immunoprecipitation (ChIP) assays were performed according to the manufacturer's instructions (Cell Signaling Technology). Briefly, 1×10^7 A549 and H460 cells were crosslinked with 1% formaldehyde, sonicated, precleared, and incubated with 10 μg Stat3 or IgG antibody per reaction. Complexes were washed with low- and high-salt buffers, and the DNA was extracted and precipitated. Precipitated DNA was amplified by real-time PCR using primers targeted PAFR promoters. Non-immunoprecipitated chromatin fragments were used as an input control.

Electrophoretic mobility shift assay

Nuclear extracts were prepared with NE-PER nuclear and cytoplasmic extraction reagents (Pierce). An electrophoretic mobility shift assay (EMSA) was performed as previously described (14). In competition experiments, 100-fold excess oligonucleotides, including PAFR-SIE, high-affinity SIE (hSIE), and irrelevant fos intragenic regulatory element (FIRE), were used. For the supershift experiment, nuclear extracts were preincubated with anti-Stat3 antibody or anti-Stat1 antibody, and IgG antibody was used as a negative control. Protein–DNA complexes were detected using a Lightshift Chemiluminescent EMSA Kit (Pierce).

PAF assay

The PAF assay was performed according to previous studies (15, 16). For analysis of PAF concentration in NSCLC cell lines, cells were washed thrice with Hank balanced salt solution. The released and the cell-associated PAF were extracted from supernatants and cells by mixing supernatants and cells in 9.5 mL of methanol, chloroform, and deionized water (2:1:0.8, v/v). Above samples mixed with chloroform (2.5 mL) and deionized water (2.5 mL) were kept at room temperature for 1 hour, and then were centrifuged (1500 × *g*, 20 minutes). The chloroform layer was aspirated and dried under nitrogen at room temperature. The residue was dissolved in 200 μL of chloroform and passed through the BondElut SI column (Amersham-Pharmacia Biotech). The column was washed with 3 mL of chloroform, 2 mL of chloroform–methanol (6:4, v/v), and 3 mL of chloroform–methanol–28% aqueous ammonia (70:85:7, v/v). PAF was eluted with 2 mL of chloroform–methanol–28% aqueous ammonia (50:50:7, v/v), and then the eluate was evaporated under nitrogen

at room temperature. The residue was finally dissolved in 200 μL of saline containing 0.1% Triton X-100. PAF concentration was analyzed using [^{3}H] PAF scintillation proximity assay (Amersham-Pharmacia Biotech). Results were expressed in picograms (pg) of PAF per 1×10^6 cells as a mean of duplicate samples.

Xenograft studies

The tumor growth of A549 and H460-cont shRNA, A549 and H460-PAFR-shRNA1, A549 and H460-PAFR-shRNA2 cells (2×10^6 cells per cell line) was determined following cell injection subcutaneously into the right flank of 6-week-old female nude mice (nu/nu mouse, Vital River Laboratories; $n = 6$ per group). Tumor sizes were calculated according to the formula: $(mm^3) = (L \times W^2) \times 0.5$ ($n = 6$ per group).The tumor metastatic ability of above cells (2×10^6 cells per cell line) was observed following cell injection intravenously into the tail vein ($n = 6$ per group). After 70 days, the mice were sacrificed and the number of metastatic nodules on the lung surface was counted. Metastatic lung were fixed with 4% paraformaldehyde before dehydration and paraffin embedding. Paraffin sections were stained with hematoxylin and eosin according to standard protocols. Animal handling and procedures were ethically approved by the Animal Center, PUMC and CAMS.

Statistical analysis

Statistical analysis was done by the Student test for simple comparisons between two groups and one-way ANOVA for comparisons among multiple groups using JMP7.0 software (SAS Institute Inc). The relationship between PAFR expression and clinicopathologic characteristic was analyzed using the χ^2 test. Survival curves were plotted by the Kaplan–Meier method and compared using the log-rank test. All data are expressed as mean ± SD. $P < 0.05$ was considered statistically significant.

Results

Upregulation of PAFR expression is associated with progression and poor prognosis of human NSCLC

To determine the clinical relevance of PAFR expression in patients with NSCLC, immunohistochemistry was used to evaluate the expression of PAFR in 150 pairs of NSCLC tumors. Immunohistochemical analysis showed that the protein levels of PAFR were significantly upregulated in 56% of NSCLC samples (84/150) as compared with adjacent normal lung tissues ($P = 0.0004$; Fig. 1A; Supplementary Table S1). Furthermore, we found that PAFR expression was positively correlated with clinical stages and TNM classification of NSCLC (Fig. 1A; Supplementary Table S2), and that NSCLC patients with high PAFR expression had shorter overall survival ($P < 0.0001$; Fig. 1B). Taken together, these results indicate that PAFR is positively correlated with poor prognosis in patients with NSCLC.

We also examined the clinical relevance of PAFR expression in patients with other types of carcinomas. PAFR exhibited high expression in breast (Supplementary Fig. S1A; Supplementary Tables S3 and S6), colorectal (Supplementary Fig. S1B; Supplementary Tables S4 and S7), and gastric (Supplementary Fig. S1C; Supplementary Tables S5 and S8) cancer tissues compared with adjacent normal tissues and PAFR expression was significantly correlated to clinical stages and TNM classification in these types of carcinomas. Consistently, high PAFR expression was associated with shorter overall survival in patients with these tumors (Supplementary Fig. S1D–S1F), respectively.

To further identify the relationship between PAFR expression and metastasis, we analyzed 30 primary tumors with matched metastatic tumors from the same patients. As shown in Fig. 1C, PAFR expression was positively correlated with distant metastasis of NSCLC. We then examined PAFR expression in other types of carcinomas with or without distant metastasis. PAFR exhibited high expression in breast (Supplementary Fig. S2A), colorectal (Supplementary Fig. S2B), and gastric cancer (Supplementary Fig. S2C) tissues compared with adjacent normal tissues and PAFR expression was clearly relevant to distant metastasis in these types of carcinomas. Collectively, these results indicate a potential role of PAFR in malignant development of human cancers. We next used NSCLC as a model to explore the function and underlying mechanisms of PAFR in promoting cancer metastasis.

Activated PAFR promotes proliferation and invasion of NSCLC cells *in vitro*

We examined PAFR expression in normal lung cells and NSCLC cells using immunoblotting. As shown in Fig. 2A, A549, H1299, H460, H157, Calu-1, or H23 exhibited higher PAFR expression compared with H441, H292, H226, Calu-3 and normal lung epithelial cell lines (BEAS-2B and NHBE). We then determined whether NSCLC cells produced their own PAF. Our results showed that PAF was synthesized in NSCLC cell lines as well as normal lung cells. Furthermore, the production level of PAF in NSCLC cell lines was significantly higher than that in normal lung cells (Supplementary Fig. S3).

To examine the oncogenic activity of PAFR in NSCLCs, we established stable retroviral expression of PAFR in H226 and Calu-3 cells (designated as H226-PAFR and Calu-3-PAFR cells), and silenced PAFR expression in A549 and H460 cells (designated as A549-shPAFR and H460-shPAFR cells). The transfection efficiency was confirmed by immunoblotting (Fig. 2B and Supplementary Fig. S4A). Compared with vector shRNA, both A549-shPAFR and H460-shPAFR cells displayed significant decreases in cell proliferation (Fig. 2C) and invasion (Fig. 2D). In contrast, H226-PAFR and Calu-3-PAFR cells exhibited significant increase in cell proliferation (Supplementary Fig. S4B) and invasive ability (Supplementary Fig. S4C) compared with control cells.

Especially, 100 nmol/L PAF incubation effectively promoted the growth and invasion of A549 and H460 cells, but could not induce the malignant development of A549-shPAFR and H460-shPAFR cells (Fig. 2C and D). In Calu-3 and H226 cells, 100 nmol/L PAF had little enhancement effect on cell growth and invasion. However, in the presence of 100 nmol/L PAF, Calu-3-PAFR, and H226-PAFR cells revealed more apparent proliferation (Supplementary Fig. S4B) and invasion (Supplementary Fig. S4C) than PAFR plasmid treatment alone. Furthermore, WEB2086, a PAFR antagonist (100 and 250 μM), suppressed A549 and H460 cell growth (Supplementary Fig. S5A) or invasion (Supplementary Fig. S5B) in a dose-dependent manner. Taken together, these results indicate the importance of the PAF/PAFR axis in the malignant development of NSCLC cells.

PAFR regulates the EMT phenotypes in NSCLC cells

EMT is the initial step of tumor invasion and metastasis, we then observed the morphologic changes and found that some A549-shPAFR and H460-shPAFR cells exhibited an epithelial-like phenotype compared with their respective control cells (Fig. 3A). Furthermore, silencing PAFR substantially increased levels of the epithelial marker (E-cadherin), decreased levels of mesenchymal

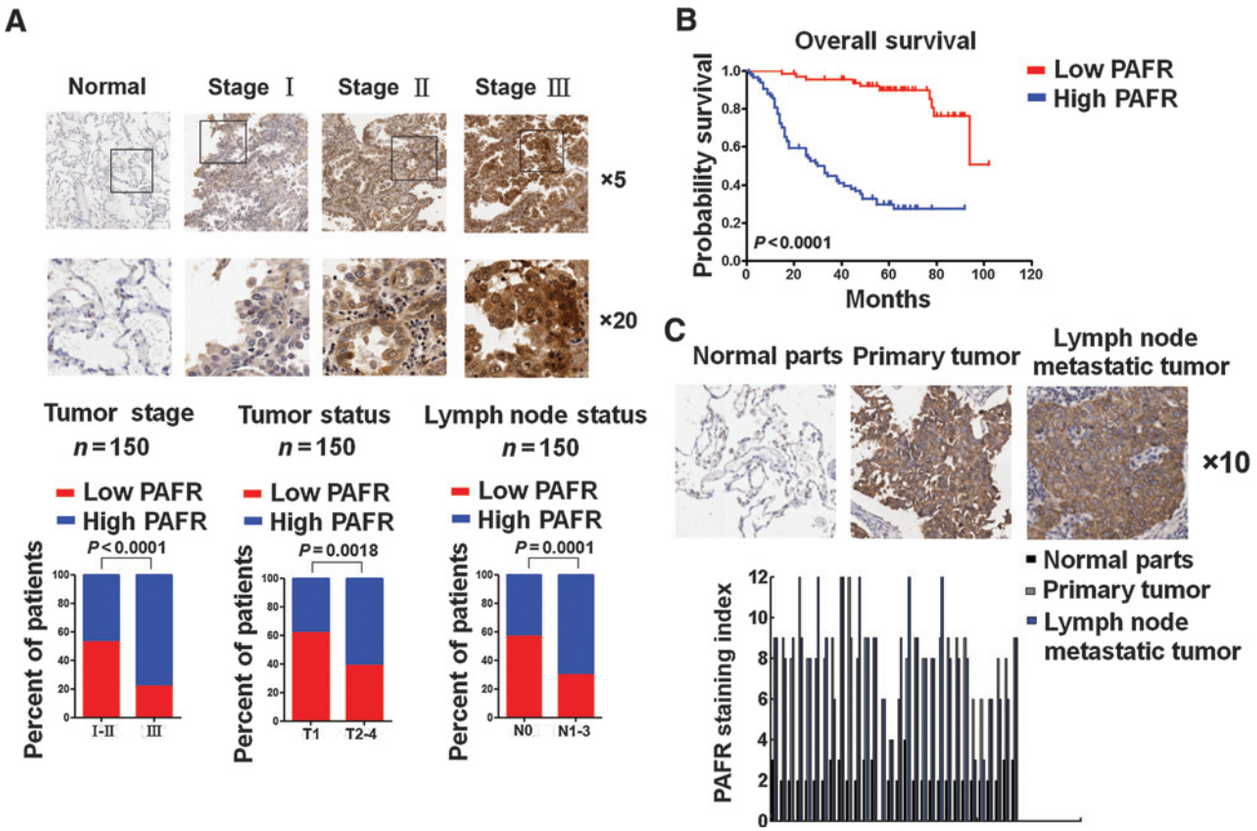

Figure 1.
PAFR positively correlates with the progression of NSCLC. A, immunohistochemical staining indicating that PAFR expression was upregulated in human NSCLC (clinical stage I–III) compared with normal lung tissue. Magnification, ×5 and ×20 as indicated. Percentage of patients (n = 150) with high expression of PAFR and low expression of PAFR according to different clinical parameters as follows: tumor stage, tumor status, and lymph node status. Two-tailed Pearson χ^2 test. B, Kaplan–Meier curves of NSCLC patients with low versus high expression of PAFR (n = 150; P < 0.0001, log-rank test). C, representative images of normal parts, lung primary tumors, and matched lymph node metastatic tumors from the same patient. The percentage of PAFR-positive cells was quantified in normal parts, lung primary tumors, and matched lymph node metastatic tumors from the same patient (n = 30). Magnification, ×10 as indicated.

markers (N-cadherin and vimentin) and EMT-related transcription factors (snail and Zeb-1) both in mRNA (Supplementary Fig. S6A and S6B) and protein (Fig. 3B) levels in A549 and H460 cells.

Conversely, H226-PAFR and Calu-3-PAFR cells exhibited fibroblastic morphology compared with their respective control cells (Supplementary Fig. S7A). This observation was further confirmed by the expression of EMT markers and EMT-related transcription factors using real-time PCR and immunoblotting analysis. PAFR overexpression greatly suppressed the expression of E-cadherin and increased the expression of N-cadherin and vimentin, as well as snail and Zeb-1 both in mRNA (Supplementary Fig. S7B) and protein (Supplementary Fig. S7C) levels in H226 and Calu-3 cells.

Especially, A549 and H460 cells incubated with 100 nM PAF displayed more spindle-like, fibroblastic morphology (Fig. 3A), and higher expression of mesenchymal markers, and lower levels of E-cadherin in A549 and H460 cells compared with control cells (Fig. 3B and Supplementary Fig. S6A and S6B). The above effects were not observed in A549-shPAFR and H460-shPAFR cells (Fig. 3A and B and Supplementary Fig. S6A and S6B). In H226 and Calu-3 cells, though PAF incubation could not induce obvious formation of fibroblastic morphology (Supplementary Fig. S7A), it resulted in slightly more levels of N-cadherin and vimentin and lower levels of E-cadherin (Supplementary Fig. S7B and S7C). However, additional PAF treatment could result in much more apparent fibroblastic morphologic changes, much higher expression of N-cadherin and vimentin while lower levels of E-cadherin in H226-PAFR and Calu-3-PAFR cells compared with PAFR plasmid treatment alone (Supplementary Fig. S7A–S7C). Therefore, these data together indicate the importance of the PAF/PAFR axis in regulating EMT in NSCLC cells, which is further supported by the observations that analyses in 90 clinical specimens showed that PAFR levels were correlated with the expression of E-cadherin (P < 0.0001), N-cadherin (P = 0.0004), vimentin (P = 0.001), snail (P = 0.003) and Zeb-1 (P = 0.03), indicating the clinical importance of PAFR in the regulation of EMT of NSCLC (Supplementary Fig. S8).

Silencing PAFR inhibits EMT in NSCLC cells mainly through inhibition of Stat3

Because Stat3 hyperactivation confers EMT of several types of cancer cells (17–19), we further examined whether Stat3 is

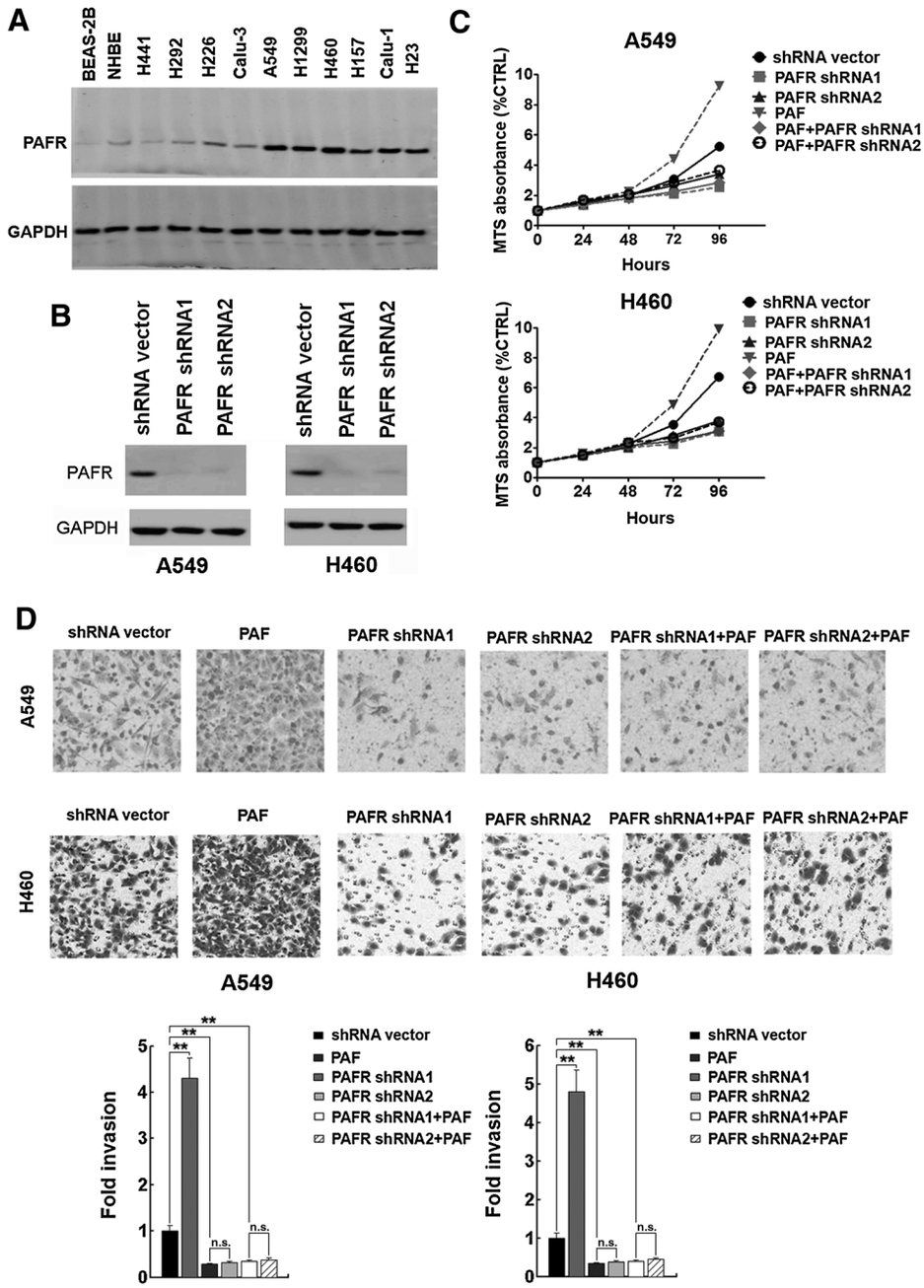

Figure 2.
The expression of PAFR in normal human lung cell lines and human NSCLC cell lines and effects of PAF/PAFR on tumor growth and invasion of A549 and H460 cells *in vitro*. A, immunoblotting analysis of PAFR proteins in normal human lung cells (BEAS-2B and NHBE) and NSCLC cell lines (H441, H292, H226, Calu-3, A549, H1299, H460, H157, Calu-1, and H23). Expression levels were normalized to GAPDH. B, transfection efficacy of PAFR shRNA plasmid in A549 or H460 cell lines was analyzed by immunoblotting, respectively. GAPDH was used as a loading control. C, Evaluating the effects of PAFR shRNA, 100 nM PAF, or 100 nM PAF in the presence of PAFR shRNA on the growth of A549 and H460 cells using MTS assay. D, evaluating the effects of PAFR shRNA, 100 nM PAF, or 100 nM PAF in the presence of PAFR shRNA on the invasion of A549 and H460 cells using Transwell invasion assay. n.s, no significant difference; **, $P < 0.01$; two-tailed unpaired Student *t* test. Error bars, mean ± SD of three independent experiments.

involved in the EMT process of NSCLC cells. As shown in Fig. 3A and B and Supplementary Fig. S6A and S6B, knockdown of Stat3 with the Stat3 shRNA markedly reduced the expression of mesenchymal markers and increased the expression of E-cadherin in A549 and H460 cells, indicating that Stat3 is also involved in the regulation of EMT in NSCLC cells.

Next, we sought to determine the role of Stat3 in the PAF/PAFR axis–mediated EMT in A549 and H460 cells. As shown in Fig. 3B and Supplementary Fig. S6A and S6B, 100 nmol/L PAF treatment could not effectively decrease the expression of E-cadherin and increased the expression of mesenchymal markers in A549-Stat3 shRNA and H460-Stat3 shRNA cells. As shown in Fig. 3A and Supplementary Fig. S9, 100 nM PAF treatment could not effectively induce obvious spindle-like, fibroblastic morphology and promote invasion of A549-Stat3 shRNA and H460-Stat3 shRNA cells. Taken together, these observations suggest that the PAF/PAFR axis regulates EMT of NSCLC cells probably dependent on the Stat3 pathway.

PAF/PAFR-induced Stat3 activation involves Src or JAK2 kinase and the autocrine IL6

We next investigated how PAFR induces Stat3 activation. Stat3 phosphorylation can be regulated by activation of kinases, such as Src and JAK2. In A549 and H460 cells, 100 nM PAF treatment

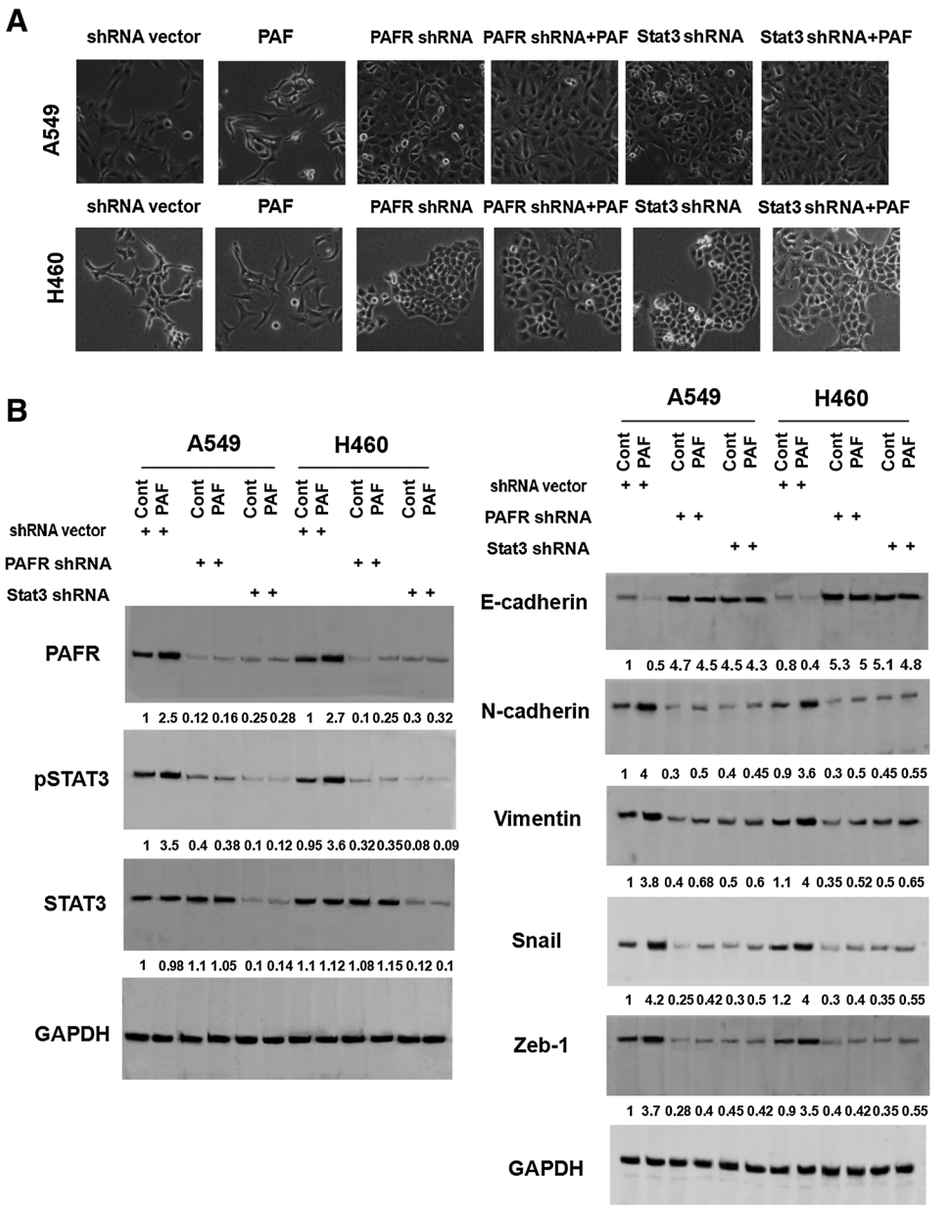

Figure 3.
Effects of the PAF/PAFR axis on Stat3-mediated EMT in A549 and H460 cells. A, morphologic changes of A549 and H460 cells harboring shRNA vector, PAFR shRNA, Stat3 shRNA, or these shRNAs in the presence of 100 nM PAF were evaluated by phase-contrast microscopy. B, immunoblotting analyses of PAFR, pStat3, or Stat3 (left) and EMT biomarkers (right) in A549 and H460 cells harboring shRNA vector, PAFR shRNA, Stat3 shRNA, or these shRNAs in the presence of 100 nM PAF. GAPDH was used as a loading control.

increased the activation of Src, JAK2, or Stat3 (Figs. 3B, left and 4A). Conversely, depletion of PAFR substantially decreased the activity of Stat3, as well as that of Src and JAK2 (Figs. 3B, left and 4B). When PAFR was depleted, additional PAF administration had no or little effect on the activities of these kinases (Figs. 3B, left and 4A).

To further investigate the involvement of Src, or JAK2 in Stat3 activation, we treated NSCLC cells with PP2, a well-characterized inhibitor of Src family kinases and AZD1480, the specific JAK2 inhibitor. PP2 (5 μM) treatment resulted in suppression of Src activation in A549 and H460 cells with or without PAF treatment. Importantly, Src inhibition was corresponded with a dramatic reduction in Stat3 phosphorylation in both cells (Fig. 4C). On the basis of these observations, we reasoned that Src activity at least partially contributes to the PAF/PAFR axis–activated Stat3. The similar results were also obtained in 1 μM AZD1480 treatment (Fig. 4C). Furthermore, either PP2 or AZD1480 did not affect the activity of JAK2 or Src, respectively. These data suggest that the PAF/PAFR axis activates Src or JAK2, leading to Stat3 activation in NSCLC cells. The PAF/PAFR axis can interact with G-proteins, especially Gαi/Gαo, and lead to activation of downstream pathways. We then used pertussis toxin, which ribosylates Gαi/Gαo in a Gαβγ heterotrimeric state-dependent fashion (20), and found that the inhibitor dose dependently (150 and 500 ng/mL) affected PAF-mediated Src or JAK2 activation, indicating that the PAF/PAFR axis activates the Stat3 pathway through a G-protein–dependent manner (Fig. 4D).

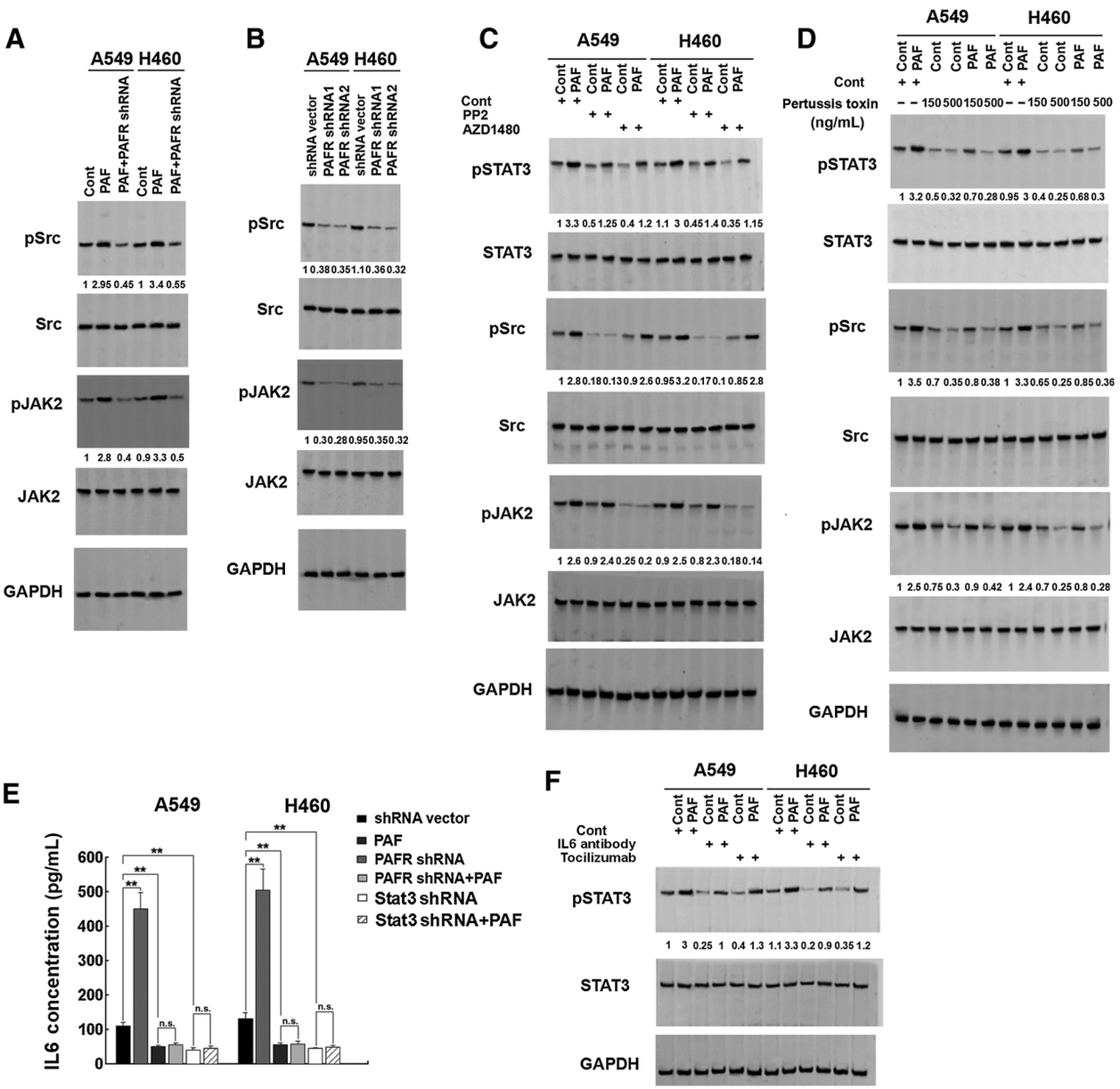

Figure 4.

PAFR-induced constitutive Stat3 activation was mediated by Src or JAK2 and the autocrine IL6. A, immunoblotting analysis of pSrc/Src or pJAK2/JAK2 ratio in PAFR-depleted A549 or H460 cells and their parental cells in the presence of 100 nmol/L PAF, respectively. Phosphoprotein blots were stripped and reprobed for their total protein counterparts. B, immunoblotting analysis of pSrc/Src or pJAK2/JAK2 ratio in shRNA vector- or PAFR shRNA-transfected A549 and H460 cells. C and D, representative immunoblots of pSrc, Src, pJAK2, JAK2, pStat3 and Stat3 from A549, H460 and A549-PAF, or H460-PAF cells treated with control solvent, PP2 (5 μM), or AZD1480 (1 μM; C) and G-protein inhibitor pertussis toxin (150 and 500 ng/mL; D). E, ELISA analyses of IL6 protein level in A549 and H460 cells harboring shRNA vector, PAFR shRNA, Stat3 shRNA, or these shRNAs in the presence of 100 nM PAF. F, Representative immunoblots of pStat3 and Stat3 from A549, H460 and A549-PAF, or H460-PAF cells treated with control solvent, 20 ng/mL IL6 antibody, or 1 μM tocilizumab. n.s, no significant difference, **, $P < 0.01$; two-tailed unpaired Student t test. Error bars, mean ± SD of three independent experiments.

Because the IL6 cytokine is a major physiologic Stat3 activator critical for Stat3-mediated oncogenesis, and given that Stat3 activation increases IL6 expression in tumors, we examined whether the PAF/PAFR axis could affect IL6 expression in NSCLC cells (21–24). As shown in Fig. 4E and Supplementary Fig. S10, 100 nM PAF incubation effectively promoted the expression of IL6 in A549 and H460 cells, but could not induce the IL6 levels in A549-shPAFR or H460-shPAFR cells and A549-shStat3 or H460-shStat3 cells. Furthermore, addition of 20 ng/mL IL6-neutralizing antibody or 1 μM IL6 receptor antagonist (tocilizumab) suppressed Stat3 activation both in A549, H460 cells and these cells stimulated with PAF (Fig. 4F). Interestingly,

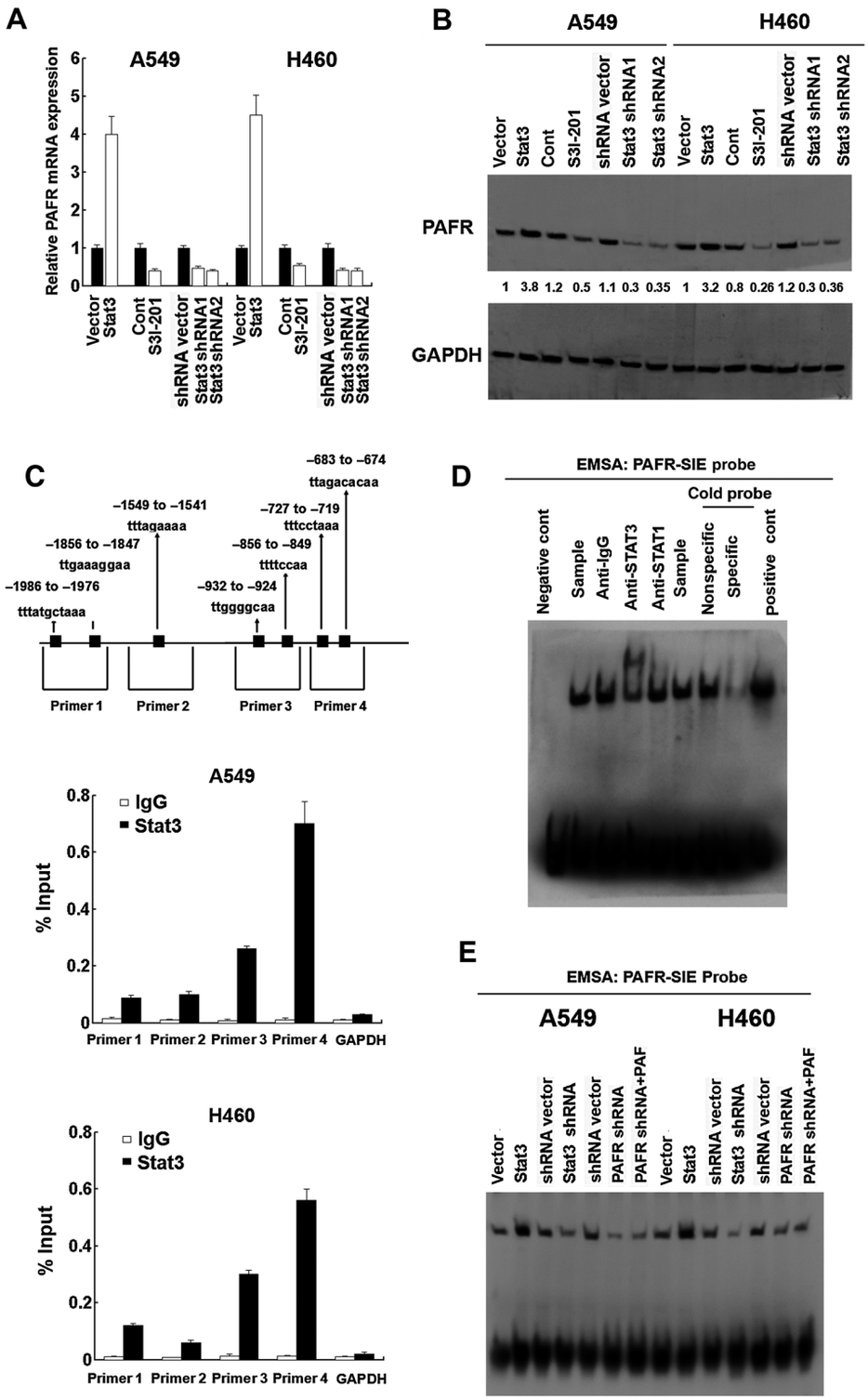

Figure 5.
The feed-forward reciprocal between Stat3 and the PAF/PAFR axis in NSCLC cells. A and B, real-time PCR (A) and immunoblotting (B) analyses of PAFR mRNA (A) or protein (B) expression in A549 and H460 cells treated with vector and Stat3 plasmid, or control solvent and 10 μM Stat3 inhibitor (S3I-201), or shRNA vector and Stat3 shRNA. C, analysis of the physical association of regions of the PAFR promoter with Stat3 by ChIP assays. Top, schematic illustration of PCR-amplified fragments of the PAFR promoter. Bottom, ChIP assays were performed in A549 and H460 cells. IgG served as the negative control. D, EMSAs with PAFR-SIE probes and nuclear extracts from H460 cells. E, Stat3–PAFR–SIE binding activity in Stat3-overexpressed NSCLC cells and Stat3-depleted, PAFR-depleted cells, or PAFR-depleted cells in the presence of 100 nM PAF compared with their respective control cells was determined by EMSA assay. Error bars, mean ± SD of three independent experiments.

the duration of Stat3 activation induced by IL6 stimulation was dramatically prolonged in PAF-treated cells and reduced in PAFR-silenced cells, indicating that the PAF/PAFR axis sustained Stat3 signaling (Supplementary Fig. S11).

Furthermore, we examined whether the PAFR/Stat3 signaling pathway in NSCLC cells was clinically relevant. As shown in Supplementary Fig. S12, PAFR level was strongly correlated with pSrc ($P = 0.0001$), pJAK2 ($P = 0.001$), pStat3 ($P < 0.0001$), and

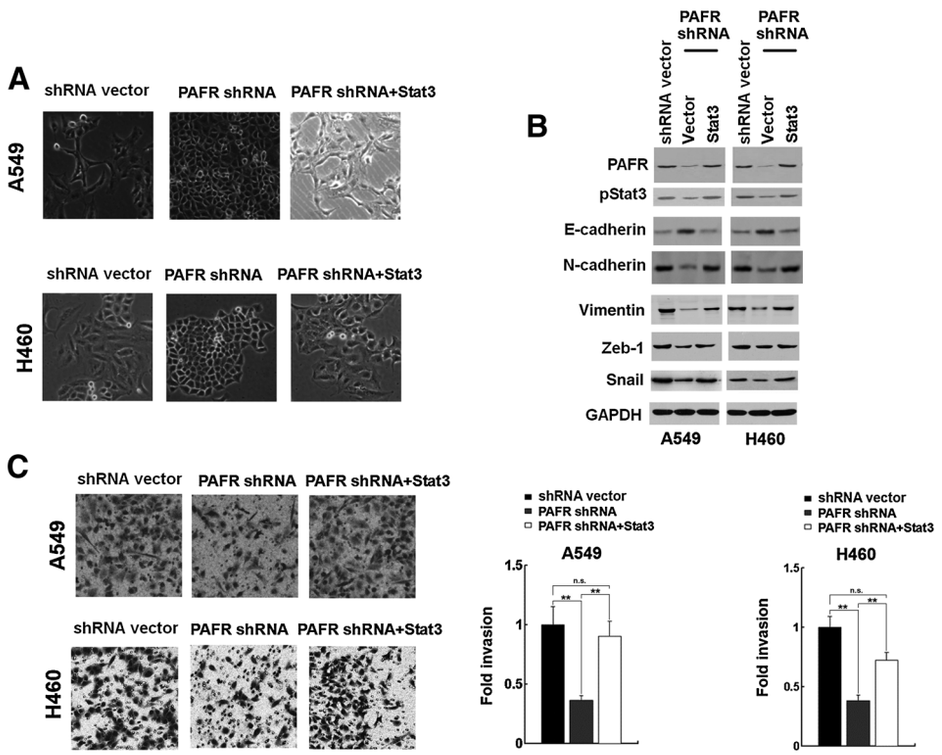

Figure 6.
Functional interplay of PAFR and Stat3 enhances the invasive potential of NSCLC cells. A, morphologic changes of A549 and H460 cells harboring PAFR shRNA alone or PAFR shRNA in the presence of Stat3 plasmid were evaluated by phase-contrast microscopy. B, Stat3 plasmid downregulated E-cadherin expression and upregulated the expression of N-cadherin, vimentin, snail, or Zeb-1 in A549-PAFR shRNA and H460-PAFR shRNA cells. C, Stat3 plasmid enhanced the invasive ability of A549-PAFR shRNA and H460-PAFR shRNA cells. n.s, no significant difference; **, $P < 0.01$; two-tailed unpaired Student t test. Error bars, mean $\pm$ SD of three independent experiments.

IL6 ($P = 0.0001$) in 90 NSCLC specimens. These results further support our *in vitro* observations that overactivated PAFR facilitates the Src and JAK2-mediated Stat3 activation and consequently leads to malignant progression and poor clinical outcomes in human NSCLC.

Stat3 positively activates the expression of PAFR in NSCLC cells

We then determined whether Stat3 affects PAFR transcription. In Fig. 5A and B, Stat3-overexpressed A549 and H460 cells displayed higher expression of PAFR both in mRNA (Fig. 5A) and protein (Fig. 5B) levels compared with control cells. Conversely, blockade of Stat3 activity with S3I-201 (10 μM) led to a markedly decrease in the expression of PAFR. Combined with the results that Stat3 depletion sufficiently reduced PAFR expression (Fig. 5A and B), these results show that Stat3 stimulates the expression of PAFR in NSCLC cells.

Given that Stat3 functions as a transcription factor, we then determined how Stat3 affects PAFR transcription. Analysis of the PAFR promoter region predicted the presence of several putative Stat3-binding sites, which harbors the core sequence TTTTGTAA. ChIP assay revealed that Stat3 most effectively bound to the fourth Stat3-binding site in the PAFR promoter, suggesting that Stat3 regulates PAFR probably through directly targeting the PAFR promoter (Fig. 5C).

Next, we performed EMSAs to evaluate the binding activity of Stat3 to the PAFR-SIE element. As shown in Fig. 5D, robust DNA binding activities were detected in H460 cells. This binding activity was largely abolished by incubating the nuclear extracts of H460 cells with Stat3 antibody, but not by anti-IgG or anti-Stat1 antibody, indicating that the majority of the PAFR-SIE binding activity consisted of Stat3 homodimers. Moreover, excess cold PAFR-SIE probes, but not an irrelevant PIRE probe, effectively impaired the binding activity in H460 cells, suggesting that the binding is PAFR-SIE specific. Stat3 overexpression or inhibition could increase or decrease the PAFR-SIE–binding ability of Stat3 (Fig. 5E). Furthermore, PAFR knockdown alone or in the presence of 100 nmol/L PAF could decrease the PAFR-SIE-binding ability of Stat3, further corroborating the reciprocal activation between the PAFR and Stat3 pathways (Fig. 5E).

PAFR and Stat3 functionally interplay in promoting the malignant development of NSCLC cells

Based on the above results, we further evaluated the biologic significance of the feed-forward reciprocal activation between PAFR and Stat3 in the EMT and invasive ability of NSCLC cells. We enforced the transfection of Stat3 plasmid to PAFR-depleted A549 and H460 cells. As Fig. 6A and B showed, Stat3 overexpression in PAFR-silenced A549 and H460 cells rescued the fibroblastic morphology and regulated the expression of EMT biomarkers. Consistent results were also obtained in Matrigel invasion assay (Fig. 6C). Combined with the results that inhibition of Stat3 activity sufficiently blocked the PAF/PAFR–promoted malignancy (Fig. 3 and Supplementary Fig. S6), these results suggest that PAFR and Stat3 functionally interplay to promote EMT and invasion of NSCLC cells.

Downregulation of PAFR inhibits growth, metastasis, and EMT of NSCLC cells *in vivo*

To extend our *in vitro* observations, we investigated whether PAFR could regulate tumor growth and metastatic capacity of NSCLC cells *in vivo*. A549-shPAFR and H460-shPAFR cells and their corresponding control cells were subcutaneously injected

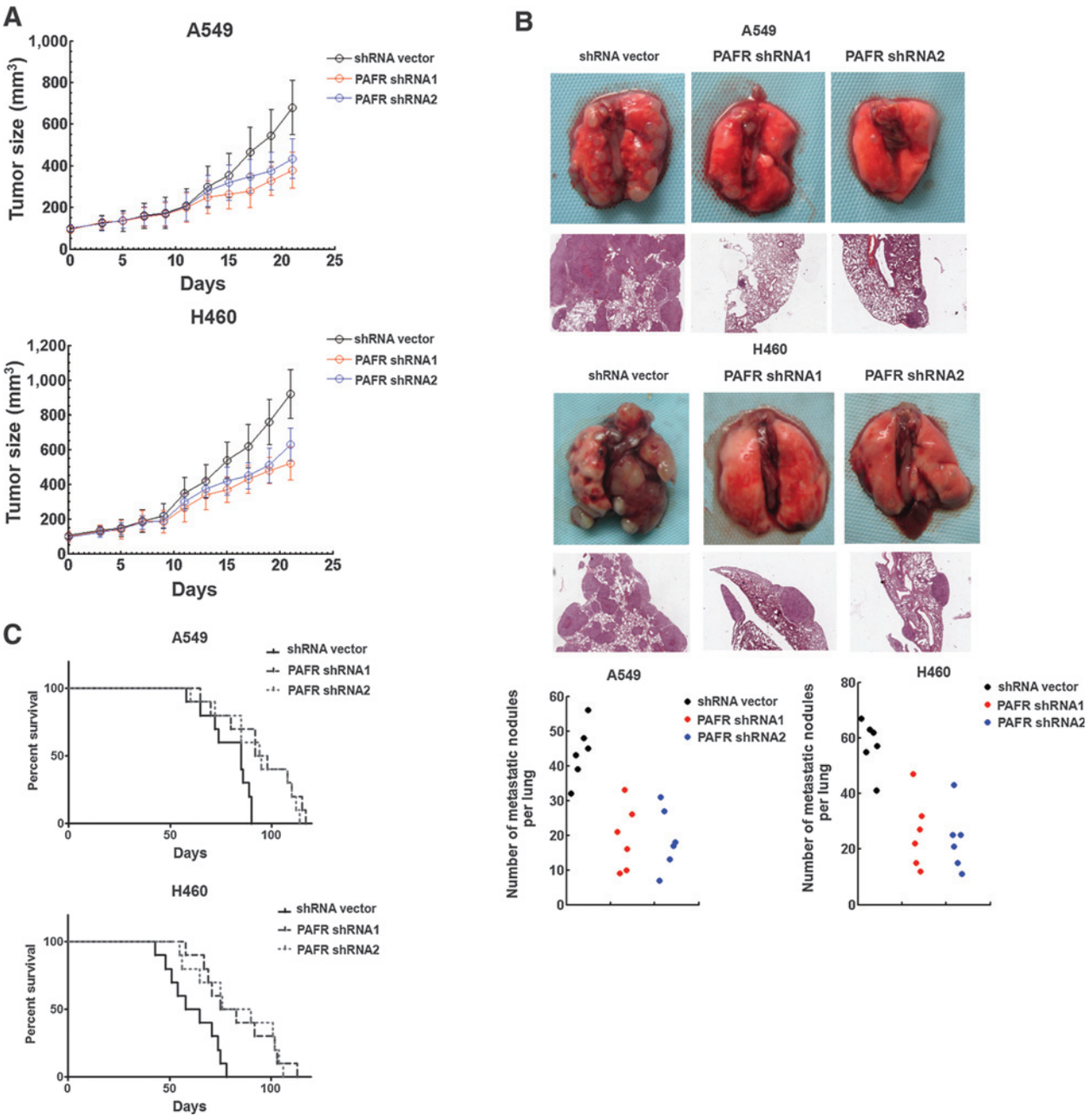

Figure 7.
Effects of PAFR depletion on growth and invasion of NSCLC cells *in vivo*. A, A549 and H460 cells stably depleting PAFR were transplanted into athymic mice ($n = 6$ per group). The growth curves of tumors are shown. Tumor size was measured every 2 days for the indicated period. The period was 21 days. B, number of metastatic nodules on the surface of the lungs of mice injected with shRNA vector or PAFR shRNA1 or 2 was presented. Representative images and H&E staining of lungs on day 70 after mice were injected with A549 and H460 stable transfectants ($n = 6$ per group). C, Kaplan–Meier curves for illustration of the survival periods of A549-shRNA vector, or A549-PAFR shRNA1 or 2, and H460-shRNA vector, or H460-PAFR shRNA1 or 2 xenografts-bearing mice.

into nude mice. As shown in Fig. 7A, the xenografts formed by PAFR-depleted cells revealed slower growth than control tumors. To further investigate the effect of PAFR shRNA on cell metastasis *in vivo*, we injected stably transfected cell lines (A549/control vector, A549/PAFR shRNA-1 or -2, H460/control vector, H460/PAFR shRNA-1 or -2) into the lateral veins of nu/nu mice and evaluated their metastatic growth in the lung. After 70 days, the PAFR shRNA-injected mice displayed a statistically significantly lower numbers of lung metastases than those injected with control shRNA cells (Fig. 7B). When lungs underwent hematoxylin and eosin staining, fewer lung metastatic nodes were observed in the mice intravenously injected with PAFR-silenced

cells compared with the control group (Fig. 7B). Furthermore, the PAFR shRNA cell–harbored mice had a significantly longer survival time compared with mice injected with control shRNA cells (Fig. 7C). Collectively, these results indicate that PAFR is necessary for the aggressive and highly metastatic phenotype of NSCLC cells. The expression of EMT markers was further observed in xenograft tumors from A549-shPAFR and H460-shPAFR cells (Supplementary Figs. S13 and S14). Consistent with the results from *in vitro* study, depletion of PAFR increased levels of E-cadherin and decreased levels of N-cadherin and vimentin.

Discussion

Increasing evidence has shown an important role of PAFR in various cancer metastases. The high expression of PAFR and its ligand PAF contributes to the liver metastasis of colorectal cancer, possibly through inducing the expression of angiogenic growth factors, VEGF and bFGF (25). Aponte and colleagues reported that overexpression and activation of PAFR upregulates MMP2 and MMP9 expression through activation of signaling networks, leading to ovarian cancer progression (9). Besides, several *in vivo* studies have shown that a variety of specific PAFR antagonists have been proven to reduce tumor metastasis (26–28). However, the comprehensive mechanisms for PAFR-mediated cancer progression remain unclear. In this study, the clinical significance of PAFR in NSCLC progression was determined, as its expression was positively correlated with malignant phenotypes of NSCLC. Moreover, silencing PAFR reduced invasion *in vitro* and inhibited metastasis of NSCLC cells *in vivo*. These studies strongly implicate that elevated PAFR promotes the progression of NSCLC. We further demonstrated that PAFR knockdown or overexpression regulated EMT biomarkers of NSCLC cells both in mRNA and protein levels. However, PAF could not effectively induce EMT and tumor malignant development in PAFR-depleted or PAFR-low expression NSCLC cells, further indicating the critical role of the PAF/PAFR axis in EMT and progression of NSCLC cells. As EMT is the initial step of tumor metastasis, these data greatly explain the PAFR-induced NSCLC metastasis and reveal a novel biologic role of PAFR in cancer malignant progression.

Although the importance of constitutive Stat3 activation in cancer has become increasingly evident, the underlying mechanisms of GPCR-induced Stat3 activation in tumors remain to be further explored (29–32). Our findings demonstrated that PAFR was capable of activating Stat3, probably through the Src tyrosine kinase. Our mechanistic analyses showed that the PAF/PAFR axis in tumor induced Stat3, in part through Gαi/o–dependent Src activation. Thus, this newly identified PAF/PAFR/Src/Stat3 axis provides the promising biomarkers for predicting the poor outcome and therapeutic targets for NSCLC treatment. Our study also demonstrates that JAK2, the downstream effector of G-proteins, contributes to PAFR-induced Stat3 activation.

Autocrine IL6 has been confirmed in various types of cancer cells, including lung cancer cells (33–36). However, comprehensive mechanisms for IL6 production in lung cancer cells is currently unclear. PAF stimulates the production of IL6 in multiple types of normal cells (37–40). However, whether the PAF/PAFR axis regulates IL6 production in cancer cells remains to be further defined. In the current study, our data show that the PAF/PAFR axis can also stimulate IL6 production in NSCLC cells. Importantly, inhibition of IL6 function effectively downregulates Stat3 activation by PAF treatment, further linking the PAF/PAFR axis to IL6 signaling in NSCLC cells.

Chronic inflammation is associated with cancer malignant progression (41). Inflammatory cells in the tumor microenvironment release cytokines to stimulate oncogenic signaling in cancer cells, including NF-κB, Stat3, and HIF1α signalings to promote cancer malignant progression (42). PAF is a potent phospholipid-derived mediator mediating a wide range of pathologic responses, including inflammation (43). It is produced by various immune and inflammatory cells, including monocytes/macrophages, neutrophils, eosinophils, basophils, and platelets (44, 45). In the current study, we found that PAF could significantly enhance NSCLC growth and metastasis via a Stat3-dependent manner. These findings strongly suggest that PAF may mediate cancer-related inflammation. IL6 is one of the most critical tumor-promoting cytokines produced by a variety of inflammatory cells in the tumor microenvironment (46). We used recombined human IL6 to mimic tumor microenvironmental IL6 and found that PAF dramatically prolonged Stat3 activation by IL6, while PAFR knockdown decreased such activation. Furthermore, the PAF/PAFR axis stimulated IL6 production in NSCLC cells. These findings suggest that PAF and IL6 produced by inflammatory cells may cooperate to promote cancer malignant progression, thus suggesting a novel mechanism for cancer-related inflammation.

The PAF/PAFR axis is critical for the secreting function of immune cells. This axis activates expression of Th17 cell cytokines, such as IL17, IL23, or IL6 and synergizes with CD36 to enhance the IL10 secretion in macrophages (47, 48). Considering that immune cells in cancer microenvironment have important functions in cancer progression through producing many cytokines (49, 50), the PAF/PAFR axis in cancer microenvironment, may also influence cancer growth and metastasis via regulating cytokine secretion in immune cells.

Furthermore, we demonstrate that Stat3-induced PAFR transcriptional activation is mediated through direct binding of Stat3 to the PAFR-SIE element in the PAFR promoter, suggesting that Stat3 is a positive regulator of PAFR expression. Together with the observations that Stat3 activation is facilitated by the PAF/PAFR axis and IL6, these data further demonstrate that the reciprocal and positive regulation between PAFR and Stat3 in the NSCLC cells. Interestingly, we observed that inhibition of either Stat3 or PAFR led to a significant reduction in invasion *in vitro* and metastasis in *vivo* in NSCLC cells, indicating that dysfunction of either Stat3 or PAFR contributes to the malignant phenotype of NSCLC. In addition, expression of exogenous Stat3 significantly reverses the suppression of invasion imposed by PAFR depletion. These findings suggest that PAFR and Stat3 can functionally interplay to augment the invasion and metastasis of NSCLC cells.

In conclusion, this study presents the pivotal finding that PAFR promotes invasion and metastasis of human NSCLC cells both *in vitro* and *in vivo* through regulating EMT, which is mainly dependent on the PAF/PAFR–stimulated Stat3 pathway and a positive reciprocal regulation between PAFR and Stat3. These findings provide insights into the underlying molecular mechanism of the malignant progression of PAFR-mediated NSCLCs (Supplementary Fig. S15). Considering that PAFR is highly expressed in NSCLC, breast, colorectal, and gastric cancers with distant metastasis, and that the vast majority of NSCLC patients succumb to their disease as a result of distant metastasis, our study suggests a

promising therapeutics target in NSCLC and probably in other types of metastatic malignant tumors.

Disclosure of Potential Conflicts of Interest

No potential conflicts of interest were disclosed.

Authors' Contributions

Conception and design: Q.-M. Zhan, J. Chen, T. Lan
Development of methodology: Q.-M. Zhan, J. Chen, T. Lan, W. Zhang
Acquisition of data (provided animals, acquired and managed patients, provided facilities, etc.): Q.-M. Zhan, J. Chen, T. Lan, W. Zhang, l. Dong
Analysis and interpretation of data (e.g., statistical analysis, biostatistics, computational analysis): Q.-M. Zhan, J. Chen, T. Lan
Writing, review, and/or revision of the manuscript: Q.-M. Zhan, J. Chen, T. Lan
Administrative, technical, or material support (i.e., reporting or organizing data, constructing databases): Q.-M. Zhan, T. Lan, W. Zhang, l. Dong, N. Kang, S. Zhang, M. Fu, B. Liu, K. Liu
Study supervision: Q.-M. Zhan

Grant Support

This work is supported by the National 973 Program (2015CB553904), the National Natural Fund of China (81230047 and 8132109), and the China Postdoctoral Science Foundation (2013M530555).

The costs of publication of this article were defrayed in part by the payment of page charges. This article must therefore be hereby marked *advertisement* in accordance with 18 U.S.C. Section 1734 solely to indicate this fact.

Received April 22, 2015; revised June 25, 2015; accepted July 29, 2015; published OnlineFirst September 10, 2015.

References

1. Muller-Tidow C, Diederichs S, Bulk E, Pohle T, Steffen B, Schwable J, et al. Identification of metastasis-associated receptor tyrosine kinases in non-small cell lung cancer. Cancer Res 2005;65:1778–82.
2. Herbst RS, Heymach JV, Lippman SM. Lung cancer. N Engl J Med 2008; 359:1367–80.
3. Dorsam RT, Gutkind JS. G-protein-coupled receptors and cancer. Nat Rev Cancer 2007;7:79–94.
4. Nikitenko LL, Leek R, Henderson S, Pillay N, Turley H, Generali D, et al. The G-protein-coupled receptor CLR is upregulated in an autocrine loop with adrenomedullin in clear cell renal cell carcinoma and associated with poor prognosis. Clin Cancer Res 2013;19:5740–8.
5. Mills GB, Moolenaar WH. The emerging role of lysophosphatidic acid in cancer. Nat Rev Cancer 2003;3:582–91.
6. Cundell DR, Gerard NP, Gerard C, Idanpaan-Heikkila I, Tuomanen EI. Streptococcus pneumoniae anchor to activated human cells by the receptor for platelet-activating factor. Nature 1995;377:435–8.
7. Melnikova VO, Villares GJ, Bar-Eli M. Emerging roles of PAR-1 and PAFR in melanoma metastasis. Cancer Microenviron 2008;1:103–11.
8. Cellai C, Laurenzana A, Vannucchi AM, Caporale R, Paglierani M, Di Lollo S, et al. Growth inhibition and differentiation of human breast cancer cells by the PAFR antagonist WEB-2086. Br J Cancer 2006;94: 1637–42.
9. Aponte M, Jiang W, Lakkis M, Li MJ, Edwards D, Albitar L, et al. Activation of platelet-activating factor receptor and pleiotropic effects on tyrosine phospho-EGFR/Src/FAK/paxillin in ovarian cancer. Cancer Res 2008;68:5839–48.
10. Radisky DC, Levy DD, Littlepage LE, Liu H, Nelson CM, Fata JE, et al. Rac1b and reactive oxygen species mediate MMP-3-induced EMT and genomic instability. Nature 2005;436:123–7.
11. Thiery JP. Epithelial-mesenchymal transitions in cancer onset and progression. Bull Acad Natl Med 2009;193:1969–78
12. Voulgari A, Pintzas A. Epithelial-mesenchymal transition in cancer metastasis: mechanisms, markers and strategies to overcome drug resistance in the clinic. Biochim Biophys Acta 2009;1796:75–90.
13. Kim WH, Chon CY, Moon YM, Kang JK, Park IS, Choi HJ. Effect of anticancer drugs and desferrioxamine in combination with radiation on hepatoma cell lines. Yonsei Med J 1993;34:45–56.
14. Epling-Burnette PK, Liu JH, Catlett-Falcone R, Turkson J, Oshiro M, Kothapalli R, et al. Inhibition of STAT3 signaling leads to apoptosis of leukemic large granular lymphocytes and decreased Mcl-1 expression. J Clin Invest 2001;107:351–62.
15. Shinozaki K, Kawasaki T, Kambayashi J, Sakon M, Shiba E, Uemura Y, et al. A new method of purification and sensitive bioassay of platelet-activating factor (PAF) in human whole blood. Life Sci 1994;54: 429–37.
16. Denizot Y, Desplat V, Drouet M, Bertin F, Melloni B. Is there a role of platelet-activating factor in human lung cancer? Lung Cancer 2001;33: 195–202.
17. Huang C, Yang G, Jiang T, Zhu G, Li H, Qiu Z. The effects and mechanisms of blockage of STAT3 signaling pathway on IL-6 inducing EMT in human pancreatic cancer cells in vitro. Neoplasma 2011;58:396–405.
18. Xiong H, Hong J, Du W, Lin YW, Ren LL, Wang YC, et al. Roles of STAT3 and ZEB1 proteins in E-cadherin down-regulation and human colorectal cancer epithelial-mesenchymal transition. J Biol Chem 2012;287: 5819–32.
19. Wendt MK, Balanis N, Carlin CR, Schiemann WP. STAT3 and epithelial-mesenchymal transitions in carcinomas. JAKSTAT 2014;3:e28975.
20. Ishii S, Shimizu T. Platelet-activating factor (PAF) receptor and genetically engineered PAF receptor mutant mice. Prog Lipid Res 2000;39:41–82.
21. Yu H, Pardoll D, Jove R. STATs in cancer inflammation and immunity: a leading role for STAT3. Nat Rev Cancer 2009;9:798–809.
22. Sumimoto H, Imabayashi F, Iwata T, Kawakami Y. The BRAF-MAPK signaling pathway is essential for cancer-immune evasion in human melanoma cells. J Exp Med 2006;203:1651–6.
23. Heinrich PC, Behrmann I, Muller-Newen G, Schaper F, Graeve L. Interleukin-6-type cytokine signalling through the gp130/Jak/STAT pathway. Biochem J 1998;334:297–314.
24. Zhong Z, Wen Z, Darnell JE Jr. Stat3: a STAT family member activated by tyrosine phosphorylation in response to epidermal growth factor and interleukin-6. Science 1994;264:95–8.
25. Denizot Y, Descottes B, Truffinet V, Valleix D, Labrousse F, Mathonnet M. Platelet-activating factor and liver metastasis of colorectal cancer. Int J Cancer 2005;113:503–5.
26. Im SY, Ko HM, Kim JW, Lee HK, Ha TY, Lee HB, et al. Augmentation of tumor metastasis by platelet-activating factor. Cancer Res 1996;56:2662–5.
27. Kang YH, Kim WH, Park MK, Han BH. Antimetastatic and antitumor effects of benzoquinonoid AC7-1 from Ardisia crispa. Int J Cancer 2001; 93:736–40.
28. Xu B, Gao L, Wang L, Tang G, He M, Yu Y, et al. Effects of platelet-activating factor and its differential regulation by androgens and steroid hormones in prostate cancers. Br J Cancer 2013;109:1279–86.
29. Kamran MZ, Patil P, Gude RP. Role of STAT3 in cancer metastasis and translational advances. Biomed Res Int 2013;2013:421821.
30. Masciocchi D, Gelain A, Villa S, Meneghetti F, Barlocco D. Signal transducer and activator of transcription 3 (STAT3): a promising target for anticancer therapy. Future Med Chem 2011;3:567–97.
31. Devarajan E, Huang S. STAT3 as a central regulator of tumor metastases. Curr Mol Med 2009;9:626–33.
32. Al Zaid Siddiquee K, Turkson J. STAT3 as a target for inducing apoptosis in solid and hematological tumors. Cell Res 2008;18:254–67.
33. Chang Q, Daly L, Bromberg J. The IL-6 feed-forward loop: a driver of tumorigenesis. Semin Immunol 2014;26:48–53.
34. Hodge DR, Hurt EM, Farrar WL. The role of IL-6 and STAT3 in inflammation and cancer. Eur J Cancer 2005;41:2502–12.
35. Bayliss TJ, Smith JT, Schuster M, Dragnev KH, Rigas JR. A humanized anti-IL-6 antibody (ALD518) in non-small cell lung cancer. Expert Opin Biol Ther 2011;11:1663–8.
36. Ancrile B, Lim KH, Counter CM. Oncogenic Ras-induced secretion of IL6 is required for tumorigenesis. Genes Dev 2007;21:1714–9.
37. Lacasse C, Turcotte S, Gingras D, Stankova J, Rola-Pleszczynski M. Platelet-activating factor stimulates interleukin-6 production by human endothelial cells and synergizes with tumor necrosis factor for enhanced

production of granulocyte-macrophage colony stimulating factor. Inflammation 1997;21:145–58.
38. Sattayaprasert P, Choi HB, Chongthammakun S, McLarnon JG. Platelet-activating factor enhancement of calcium influx and interleukin-6 expression, but not production, in human microglia. J Neuroinflammation 2005;2:11.
39. Ichinowatari G, Yamada M, Yaginuma H, Tsuyuki K, Tanimoto A, Ohuchi K. Participation of prostaglandin E2 and platelet-activating factor in thapsigargin-induced production of interleukin-6. Eur J Pharmacol 2002;434:187–96.
40. Gaumond F, Fortin D, Stankova J, Rola-Pleszczynski M. Differential signaling pathways in platelet-activating factor-induced proliferation and interleukin-6 production by rat vascular smooth muscle cells. J Cardiovasc Pharmacol 1997;30:169–75.
41. Coussens LM, Werb Z. Inflammation and cancer. Nature 2002;420:860–7.
42. Mantovani A, Allavena P, Sica A, Balkwill F. Cancer-related inflammation. Nature 2008;454:436–44.
43. Stafforini DM, McIntyre TM, Zimmerman GA, Prescott SM. Platelet-activating factor, a pleiotrophic mediator of physiological and pathological processes. Crit Rev Clin Lab Sci 2003;40:643–72.
44. Braquet P, Rola-Pleszczynski M. The role of PAF in immunological responses: a review. Prostaglandins 1987;34:143–8.
45. Camussi G, Tetta C, Baglioni C. The role of platelet-activating factor in inflammation. Clin Immunol Immunopathol 1990;57:331–8.
46. Lin WW, Karin M. A cytokine-mediated link between innate immunity, inflammation, and cancer. J Clin Invest 2007;117:1175–83.
47. Fillon S, Soulis K, Rajasekaran S, Benedict-Hamilton H, Radin JN, Orihuela CJ , et al. Platelet-activating factor receptor and innate immunity: uptake of gram-positive bacterial cell wall into host cells and cell-specific pathophysiology. J Immunol 2006;177:6182–91.
48. Rios FJ, Ferracini M, Pecenin M, Koga MM, Wang Y, Ketelhuth DF , et al. Uptake of oxLDL and IL-10 production by macrophages requires PAFR and CD36 recruitment into the same lipid rafts. PLoS One 2013;8:e76893.
49. Holzel M, Bovier A, Tuting T. Plasticity of tumour and immune cells: a source of heterogeneity and a cause for therapy resistance? Nat Rev Cancer 2013;13:365–76.
50. Balkwill F. Cancer and the chemokine network. Nat Rev Cancer 2004;4:540–50.